# Analysis of water dynamics in the soil-plant continuum using a multi-sensor approach

EGU General Assembly 2020

D. Chaparro, T. Jagdhuber, M. Piles, D. Entekhabi, A. Fluhrer, A. Feldman, F. Jonard, M. Vall-llossera, A. Camps

@Dchaparro_EO @Maria_Piles #shareEGU20

UNIVERSITAT POLITÈCNICA DE CATALUNYA BARCELONATECH

DLR

VNIVERSITAT DE VALÈNCIA

EGU General Assembly 2020

# 1. Water in soil and vegetation from satellites

**Objective: understanding the water pools and fluxes in the soil-plant continuum (SPC)**

- Water content in soils: soil moisture from passive microwave remote sensing (L-band)
- Water content in vegetation:
  - Vegetation water content (VWC; $kg/m^2$): water per unit area.
  - **Gravimetric vegetation moisture (Mg; kg/kg): water per wet biomass →** **Monitor water status: today's presentation**

**VWC** - Linked to biomass

Empirical approach: link VOD to VWC using the *b*-parameter (from land cover data)

$$VOD = b \cdot VWC$$

**Mg** - Linked to **water status**

Physically based approach[1]: link VOD and Mg

$$VOD = 4\pi \left(\frac{VH}{\lambda}\right) \cdot Im[\sqrt{\varepsilon_{can}}]$$

$$\varepsilon_{can} = \varepsilon_{air}\left(1 + 3\delta \frac{(\varepsilon_{veg} - \varepsilon_{air})}{(\varepsilon_{veg} + 2 \cdot \varepsilon_{air})}\right)$$

$$\varepsilon_{veg} = f(Mg)$$ Ulaby & El Rayes, 1987

[1]Fink et al., 2018

➢ A **multi-sensor approach** (Fink et al., 2018) is applied to retrieve Mg and sense vegetation **water status**:

Step 1: model VOD from δ and VH

**Lidar-Derived Vegetation Height**
***VH* [m]**

**Radar-Derived Vegetation Vol. Fraction**
***δ***

⬇ ⬇

$VOD$-Model

$$VOD = 4\pi\left(\frac{VH}{\lambda}\right)\cdot Im\left[\sqrt{\varepsilon_{air}\left(1+3\delta\frac{(\varepsilon_{veg}-\varepsilon_{air})}{(\varepsilon_{veg}+2\cdot\varepsilon_{air})}\right)}\right]$$

$\varepsilon_{air} = 1$

➢ A **multi-sensor approach** (Fink et al., 2018) is applied to retrieve Mg and sense vegetation **water status**:

**Lidar-Derived Vegetation Height**
**$VH$ [m]**

**Radar-Derived Vegetation Vol. Fraction**
**$\delta$**

$VOD$-Model

$$VOD = 4\pi \left(\frac{VH}{\lambda}\right) \cdot Im\left[\sqrt{\varepsilon_{air}\left(1 + 3\delta \frac{(\varepsilon_{veg} - \varepsilon_{air})}{(\varepsilon_{veg} + 2 \cdot \varepsilon_{air})}\right)}\right]$$

$\varepsilon_{air} = 1$

**Radiometer-Derived VOD**

Step 2: compare modelled vs retrieved VODs.

$$\boldsymbol{min\left(\left|VOD_{Model} - VOD_{Radiometer}\right|\right)}$$

$$\hookrightarrow \boldsymbol{\varepsilon_{veg}}$$

- A **multi-sensor approach** (Fink et al., 2018) is applied to retrieve Mg and sense vegetation **water status**:

**Lidar-Derived Vegetation Height**
$\boldsymbol{VH}$ **[m]**

**Radar-Derived Vegetation Vol. Fraction**
$\boldsymbol{\delta}$

$VOD$-Model

$$VOD = 4\pi\left(\frac{VH}{\lambda}\right)\cdot Im\left[\sqrt{\varepsilon_{air}\left(1+3\delta\frac{(\varepsilon_{veg}-\varepsilon_{air})}{(\varepsilon_{veg}+2\cdot\varepsilon_{air})}\right)}\right]$$

$\varepsilon_{air} = 1$

**Radiometer-Derived VOD**

$$\boldsymbol{min\left(\left|VOD_{Model} - VOD_{Radiometer}\right|\right)}$$
$\boldsymbol{\hookrightarrow \varepsilon_{veg}}$

Ulaby and El-Rayes, 1987

$M_g\,[\mathrm{kg/kg}]$

Step 3: estimate Mg

# 2. Datasets used for Mg retrievals

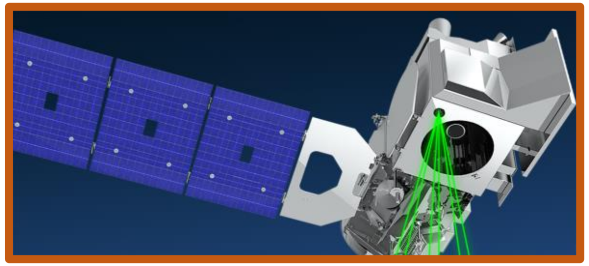

ICESat-2

**Vegetation height (VH)** – Maximum (TOC)

- ➢ICESat-2 VH (October 2018 – September 2019) – New VH data
- ➢VH from Simard et al. (2011; derived from ICESat-1 & auxiliary variables) – Reference data

**Result of final VH product**

**VH max (ICESAT2)** **VH max (ICESAT1 - Simard et al.)**

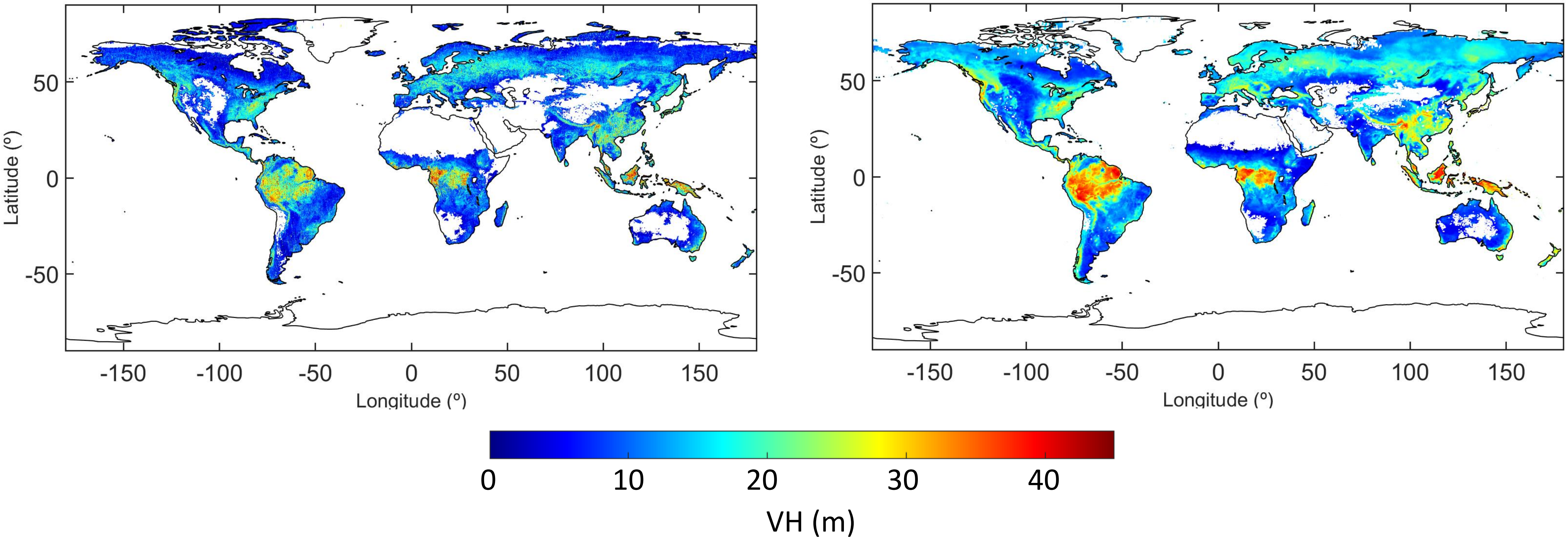

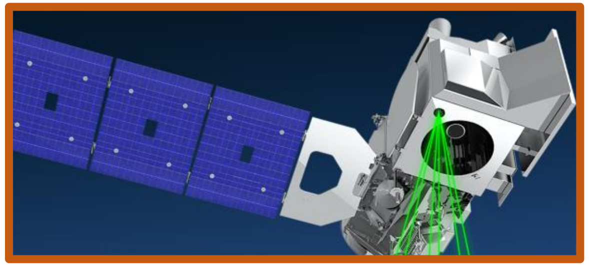


**Vegetation height (VH)** – Maximum (TOC)

- ICESat-2 VH (October 2018 – September 2019) – New VH data
- VH from Simard et al. (2011; derived from ICESat-1 & auxiliary variables) – Reference data

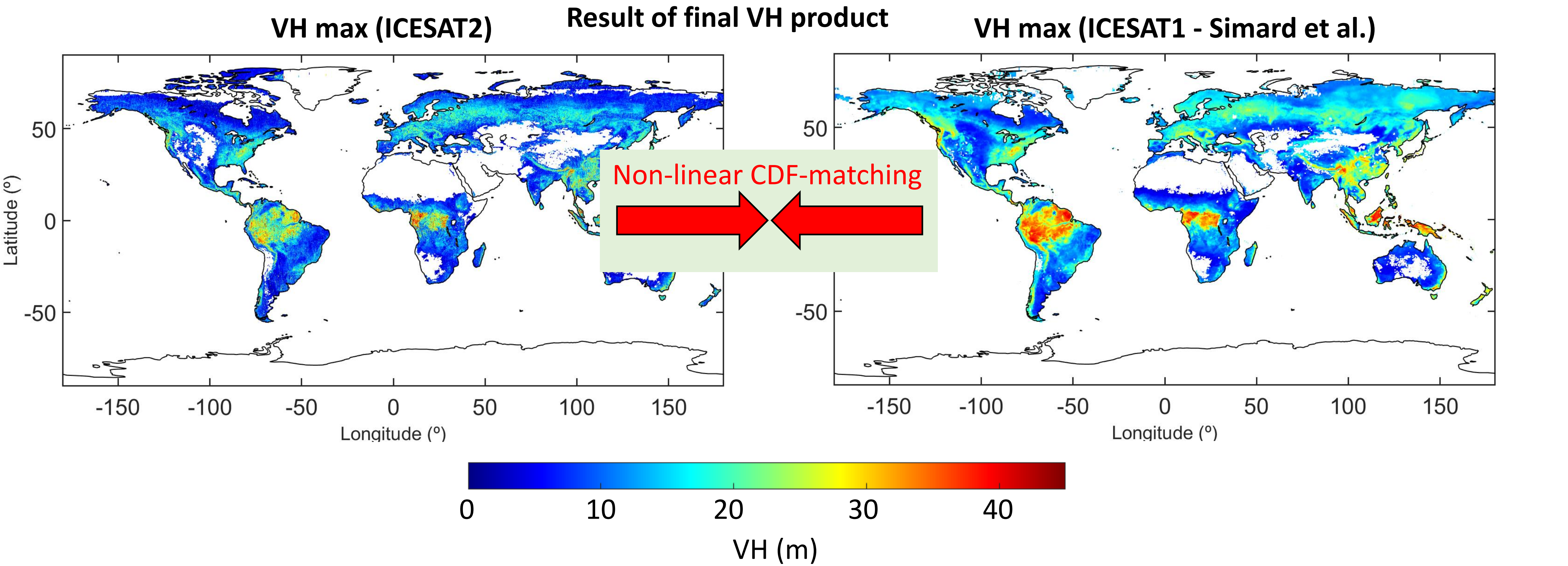

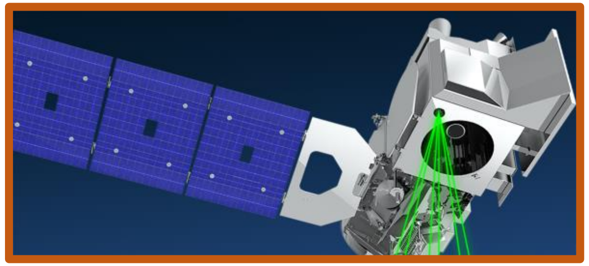

ICESat-2

**Vegetation height (VH)** – Maximum (TOC)

➢ICESat-2 VH (October 2018 – September 2019) – New VH data

➢VH from Simard et al. (2011; derived from ICESat-1 & auxiliary variables) – Reference data

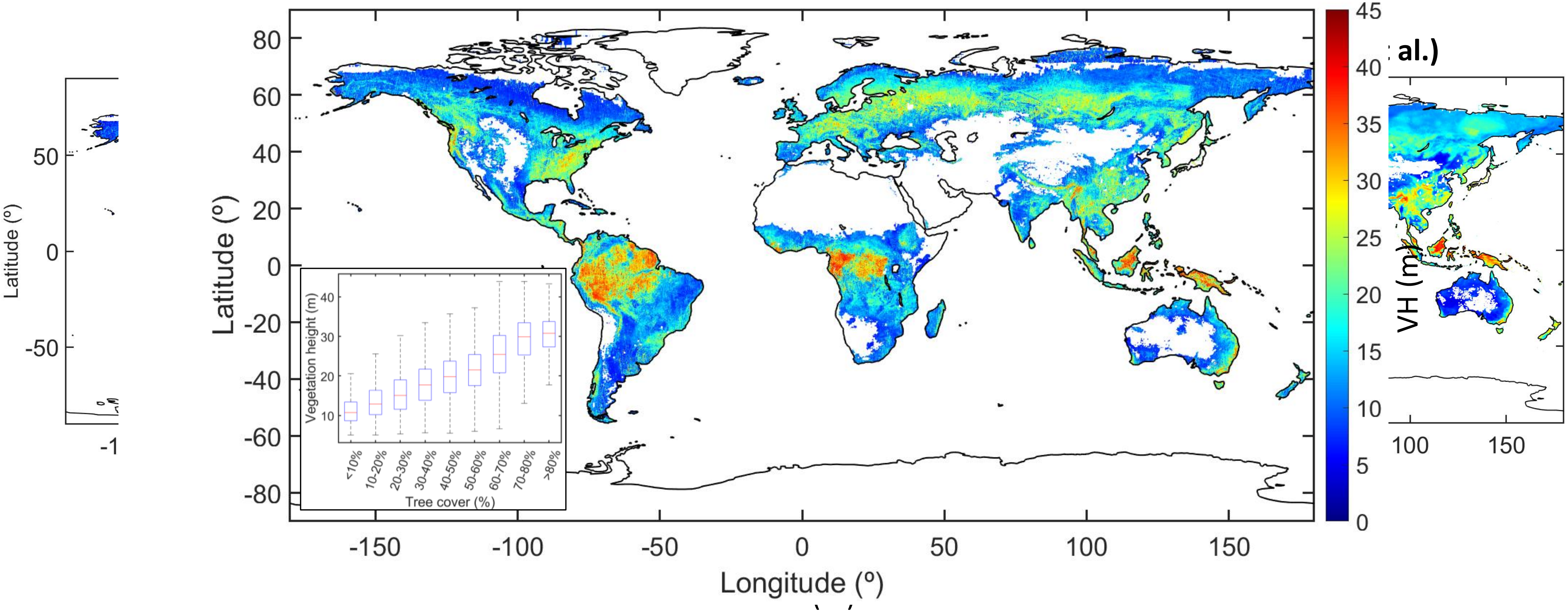

## Vegetation volume fraction (δ)

- Aquarius radar (2011-2014) – A δ seasonality is built → dynamic variable
- δ derives from the Radar Vegetation Index (RVI):

$$RVI = \frac{8 \cdot \sigma_{HV}}{\sigma_{HH} + \sigma_{VV} + 2 \cdot \sigma_{HV}} \qquad \delta = 0.01 \cdot RVI$$

- δ shows the vegetation structure:

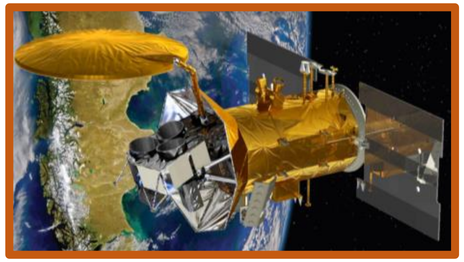

Aquarius

Delta shows the vegetation volume fraction [m3/m3] recognized by an L-band radar. It is obtained by rescaling the radar vegetation index (RVI; Fink et al., 2018)

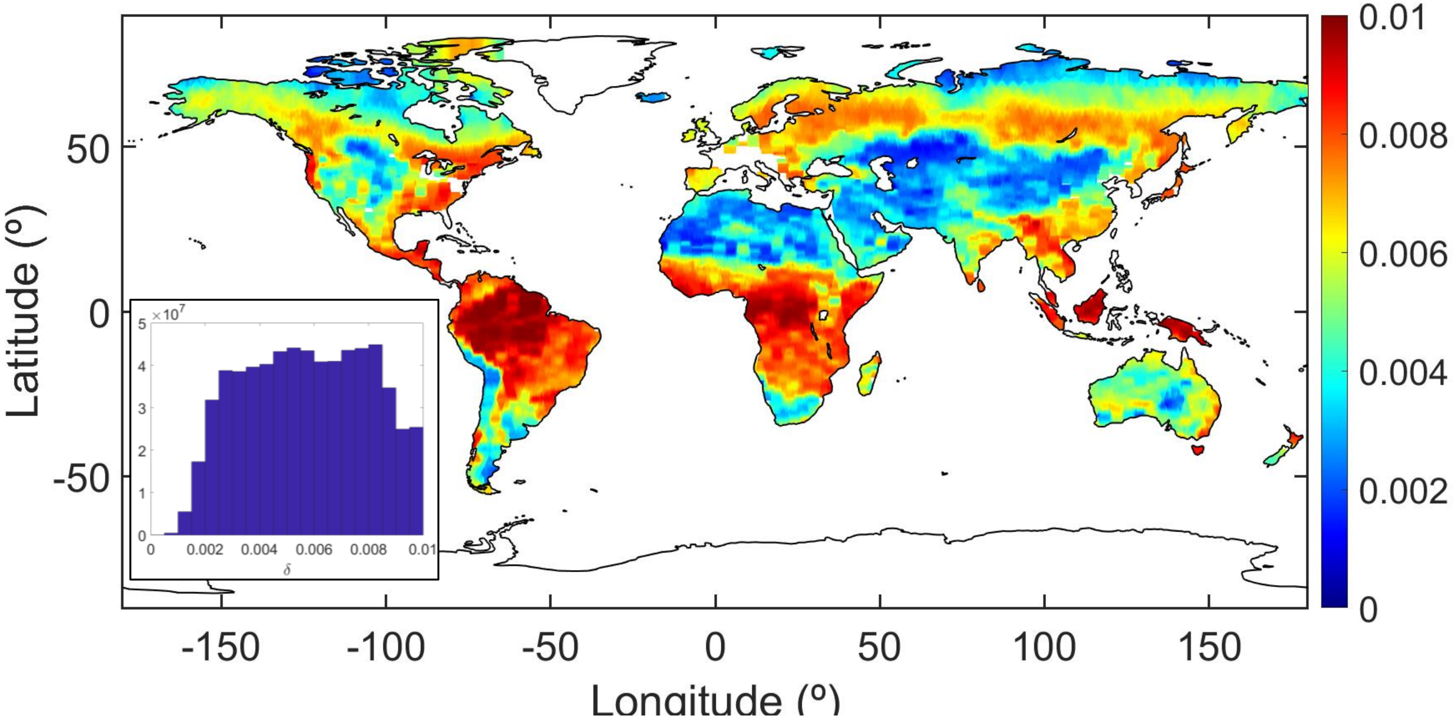


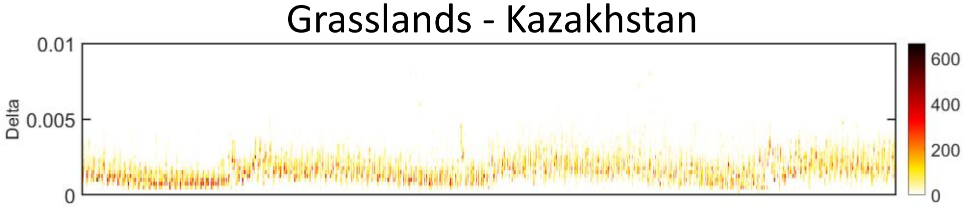


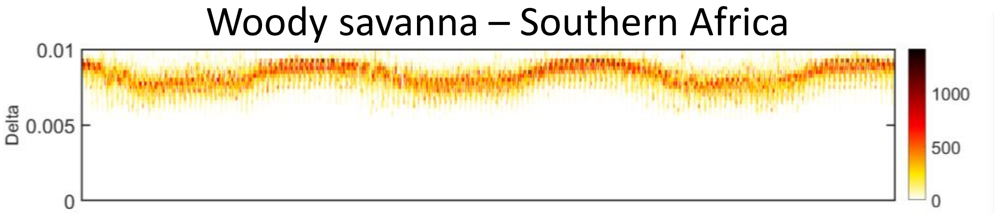


Examples of δ time-series for the Aquarius period. Colorbars show the number of pixels for each bin of the histogram.

## Vegetation Optical Depth (VOD)

- SMAP VOD (2015-2019); retrieval algorithm: MT-DCA (Konings et al., 2016).
- Radiometer-deried VOD is compared to modelled VOD: then Mg is obtained

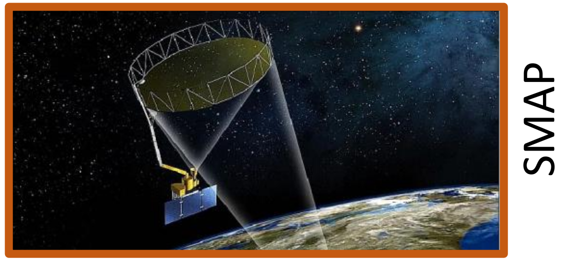


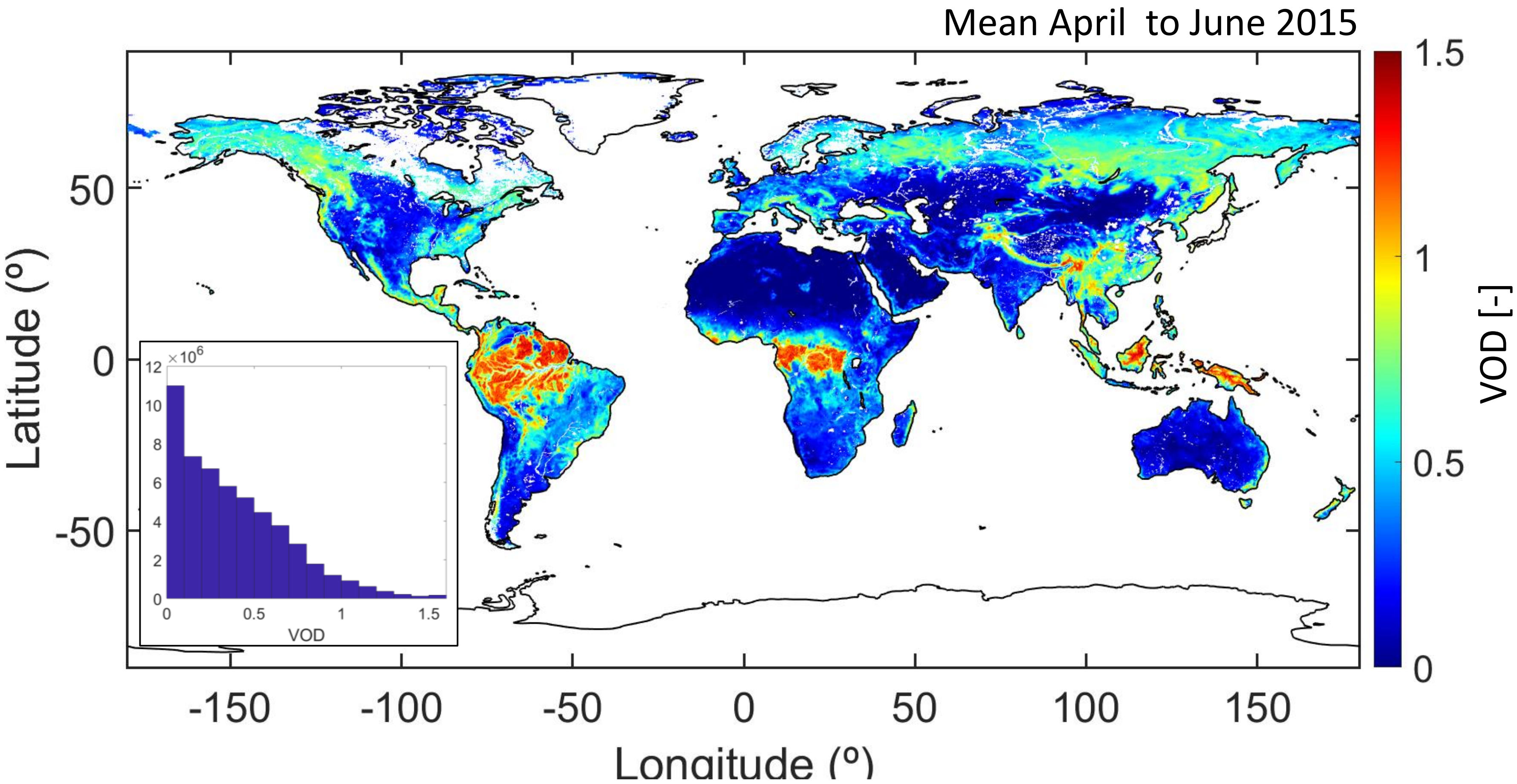

# 3. Resulting Mg maps

- Mg maps for the period April 2015 – September 2019 have been obtained.
- Examples:

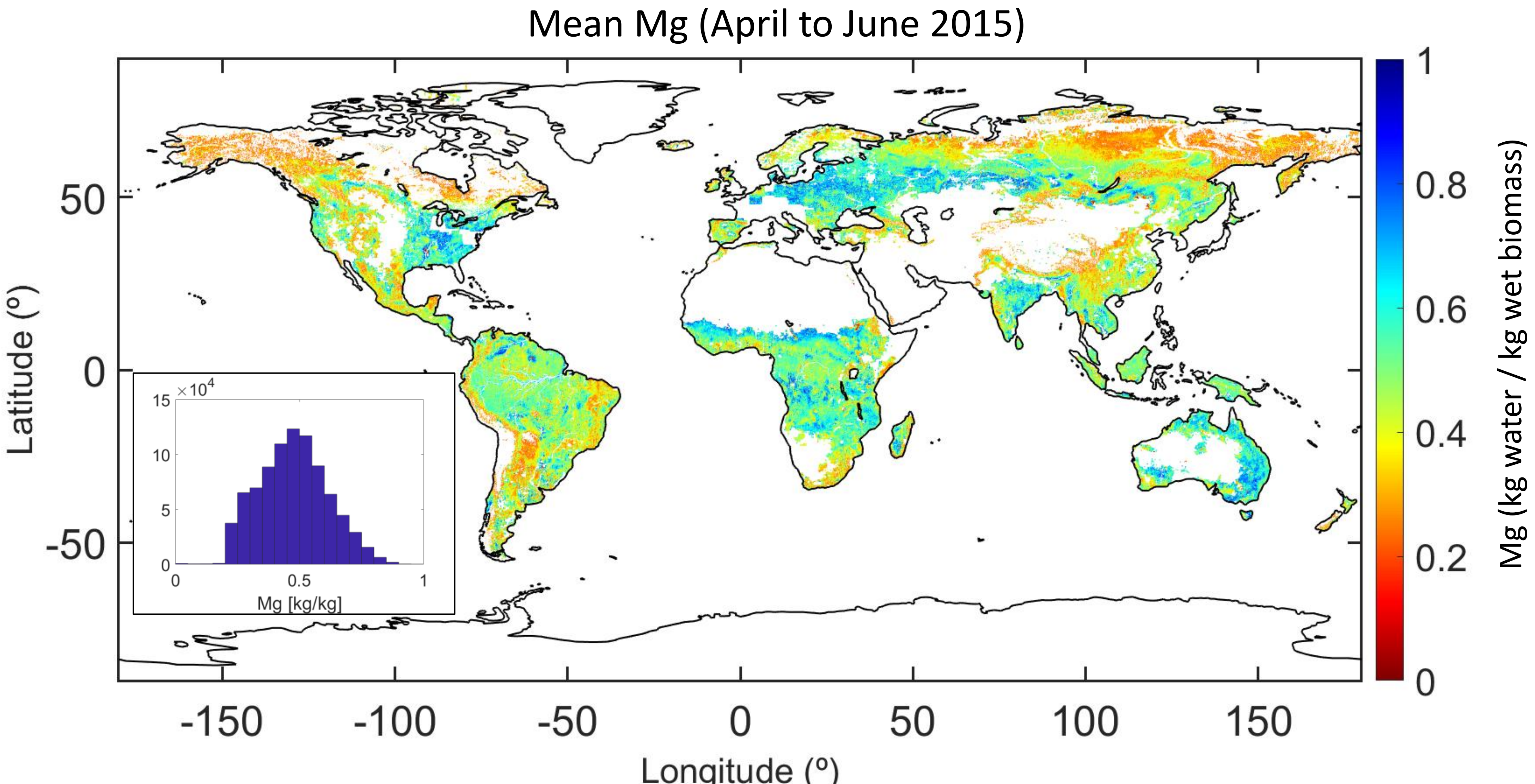

➢Mg maps for the period April 2015 – September 2019 have been obtained.

➢Examples:

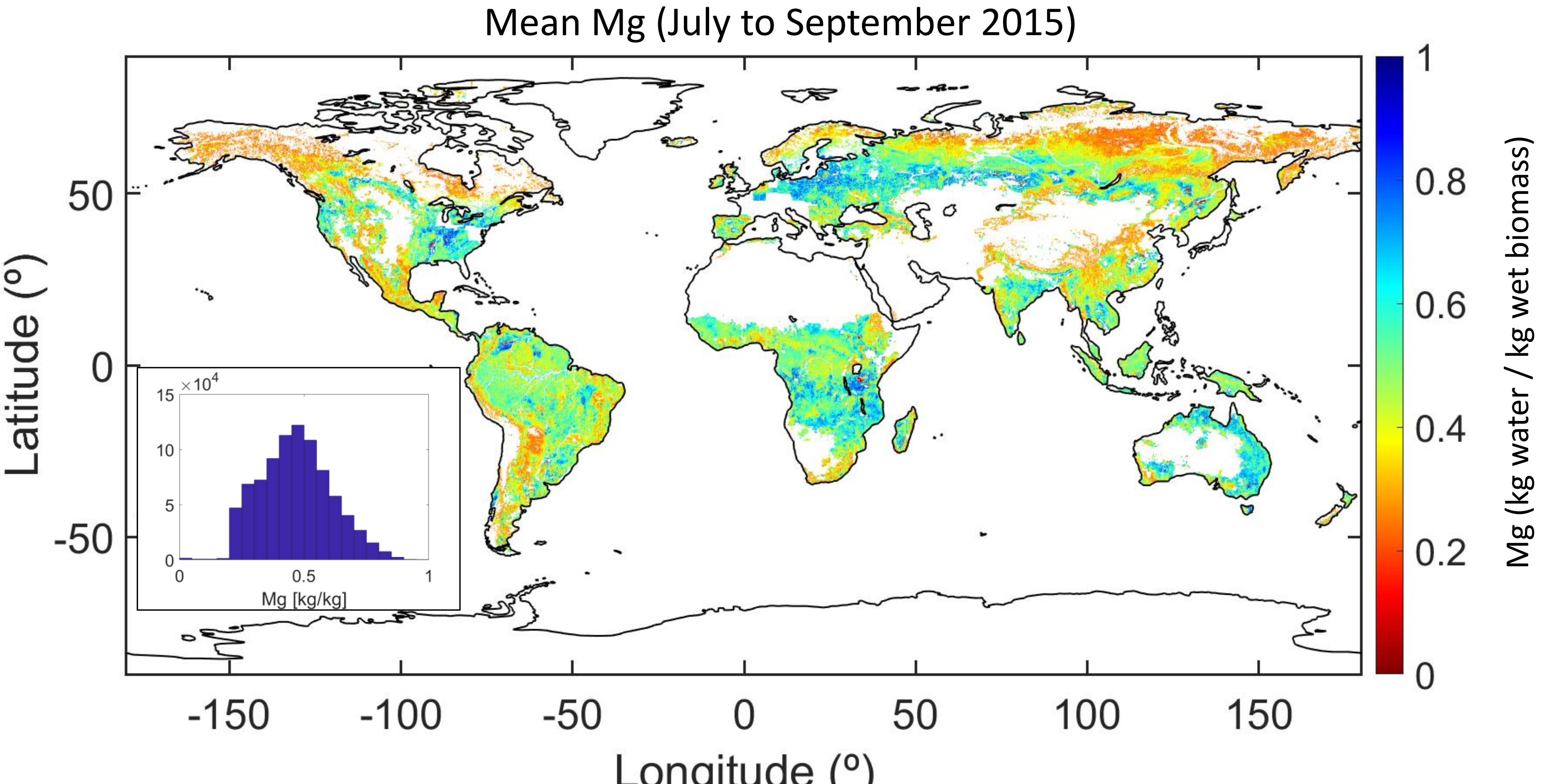

➢Mg maps for the period April 2015 – September 2019 have been obtained.

➢Examples:

Differences (Mean JulSep – Mean AprJun)

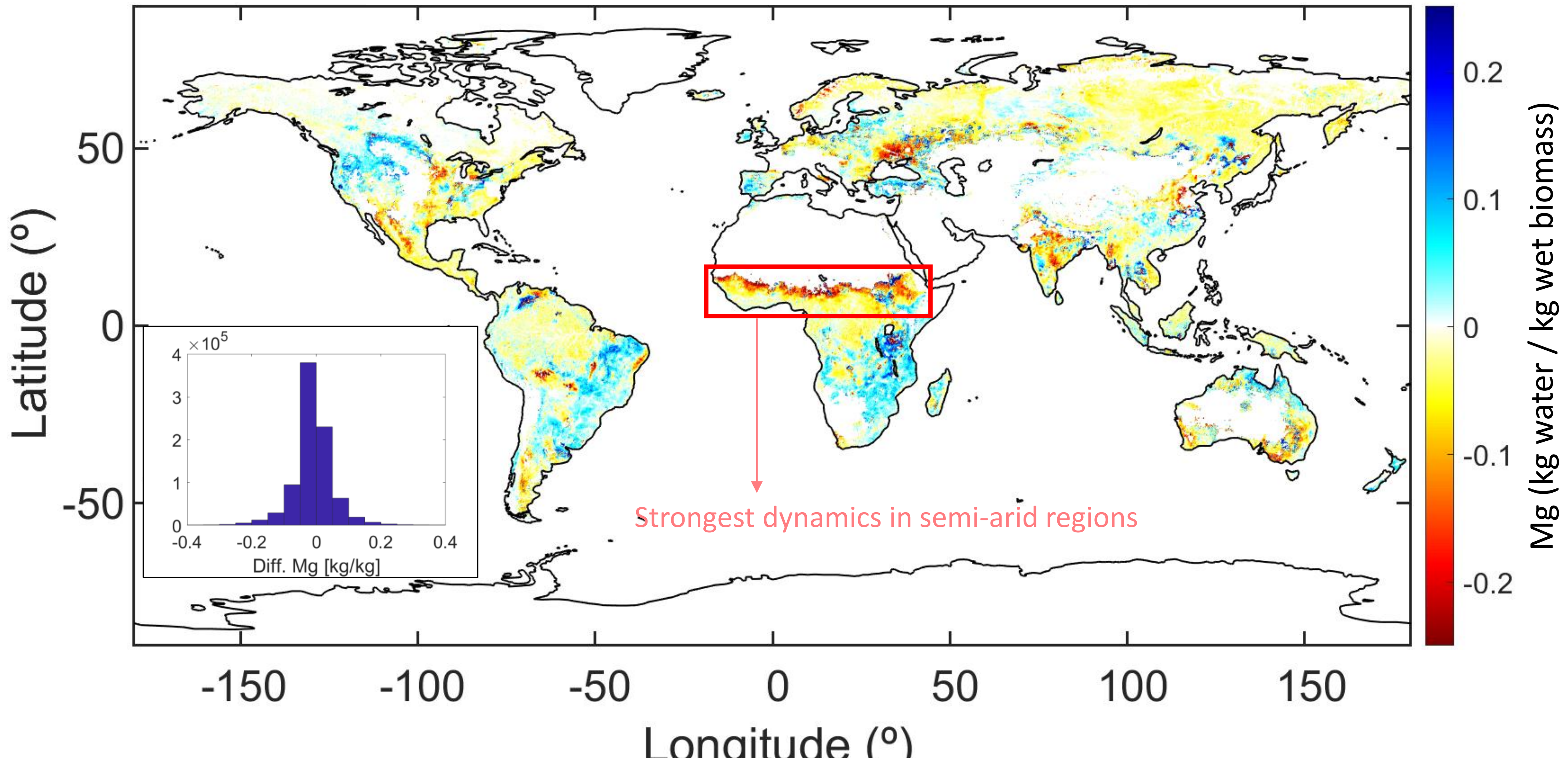

# 4. Study case: woody savanna in California

- Ongoing work: first time-series analyses in California.
- Pixels chosen (n=27) with (i) homogeneous IGBP “woody-savanna” & (ii) warm temperate, hot/dry summer climate (Csa category in Koppen-Geiger classification; Beck et al., 2018).

**Complementary datasets**

- Leaf Area Index (MODIS LAI; product MOD15A2H).
- Soil Moisture (SMAP SM; 9 km gridding; MT-DCA retrievals[2]).
- Vegetation volume fraction ($\delta$; Aquarius) climatology.
- All datasets aggregated at 9 km SMAP gridding.
- All datasets smoothed (91 d. mov. avg.) to study seasonality.

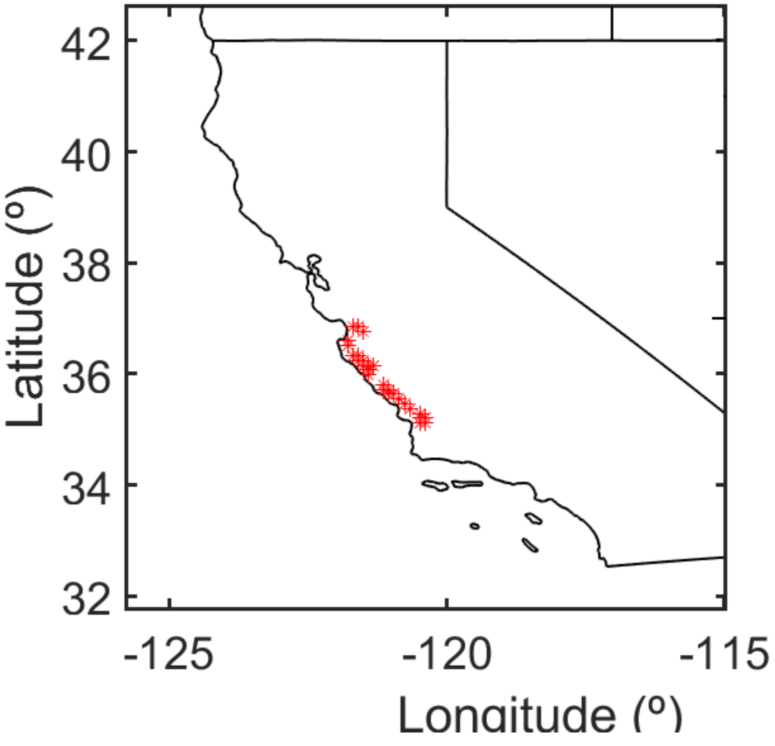


* Pixels studied in California

[2] Konings et al., 2016

➢ Comparison of Mg with SM, LAI, VOD and δ time-series:

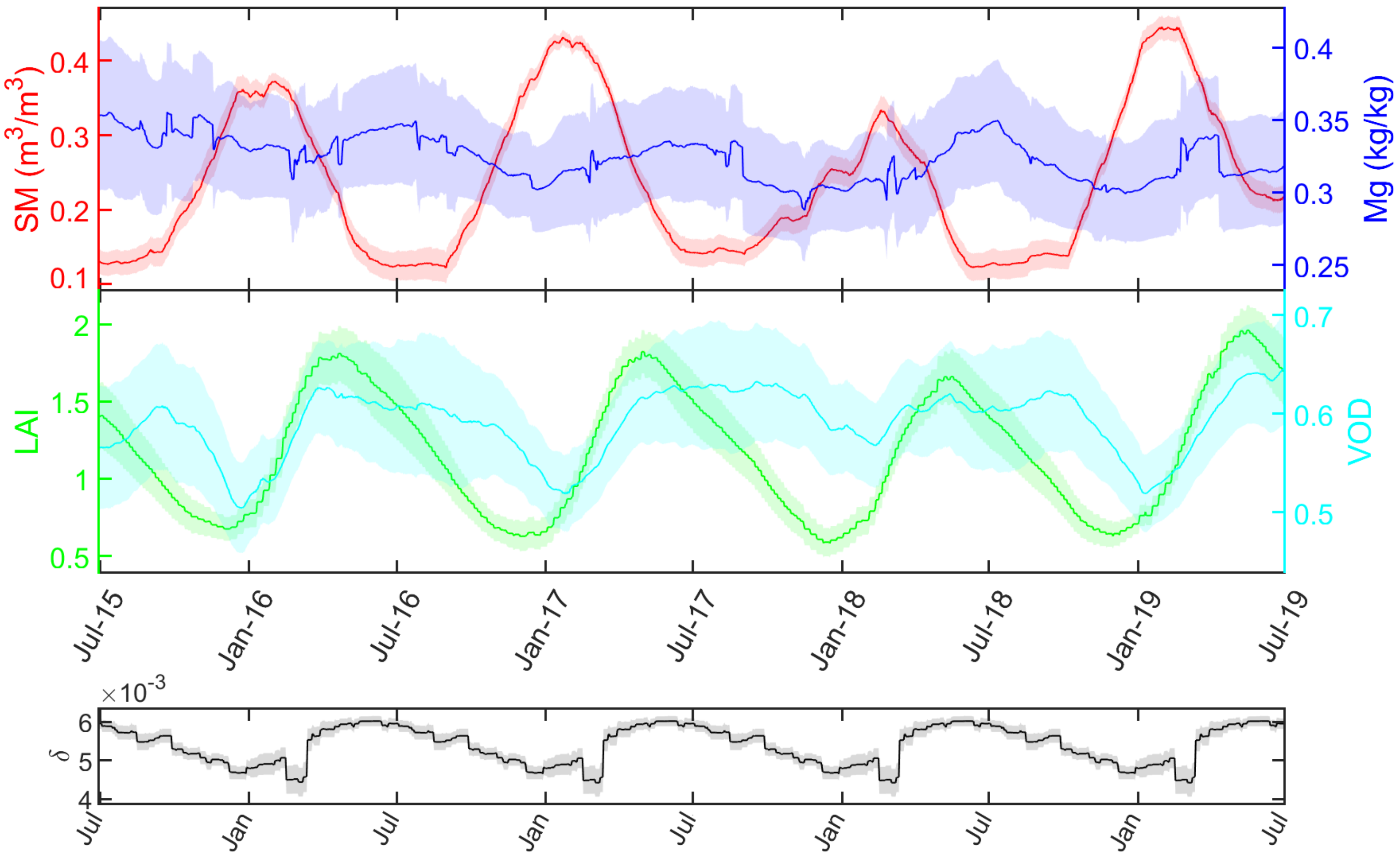


❖ Increasing SM precedes leaf growth (LAI) and structure changes (δ).

❖ Mg increases after LAI-δ peaks, suggesting water uptake after leaves growth.

❖ VOD high plateau during LAI & Mg maxima affirming double sensitivity of VOD (biomass & plant water)

➢ Comparison of Mg with SM, LAI, VOD and δ time-series:

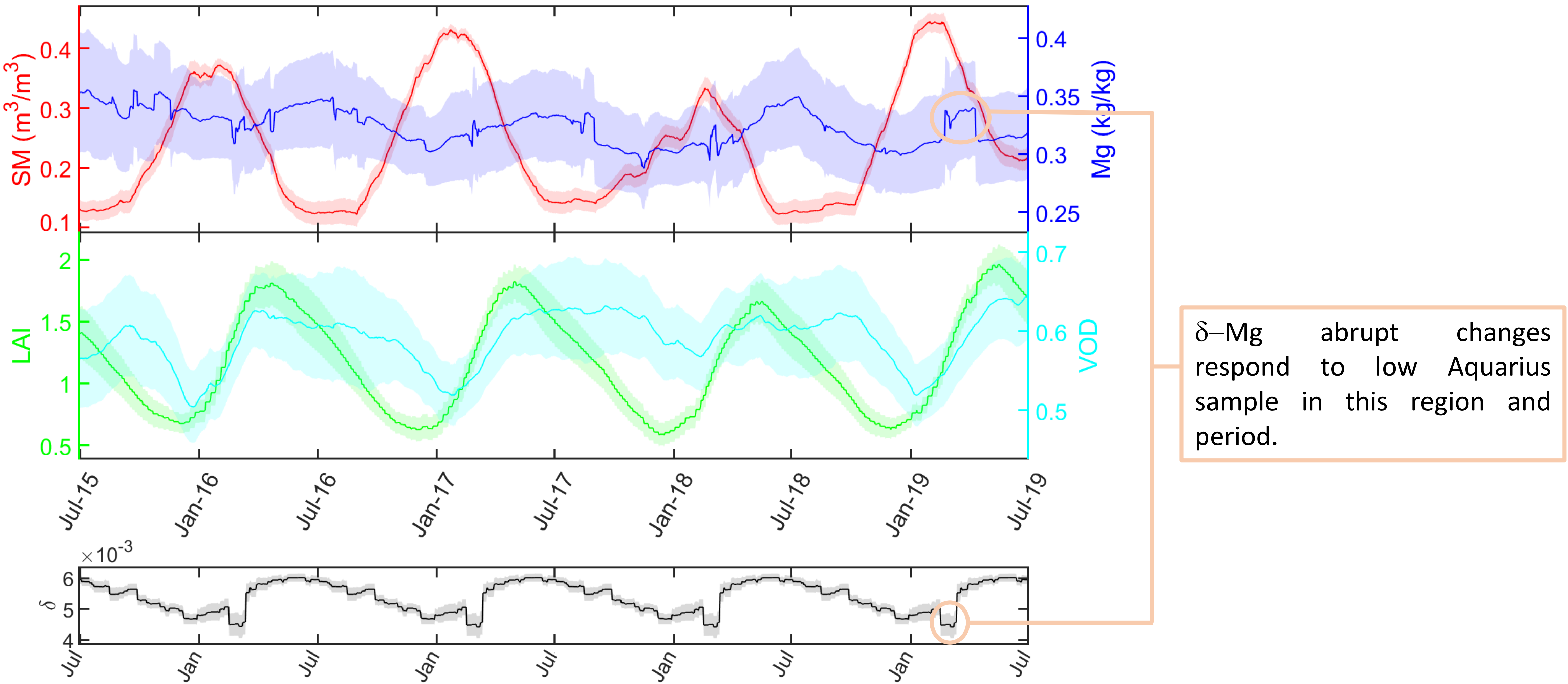


❖ Increasing SM precedes leaf growth (LAI) and structure changes (δ).

❖ Mg increases after LAI-δ peaks, suggesting water uptake after leaves growth.

❖ VOD high plateau during LAI & Mg maxima affirming double sensitivity of VOD (biomass & plant water)

➢ Comparison of Mg with SM, LAI, VOD and δ time-series:

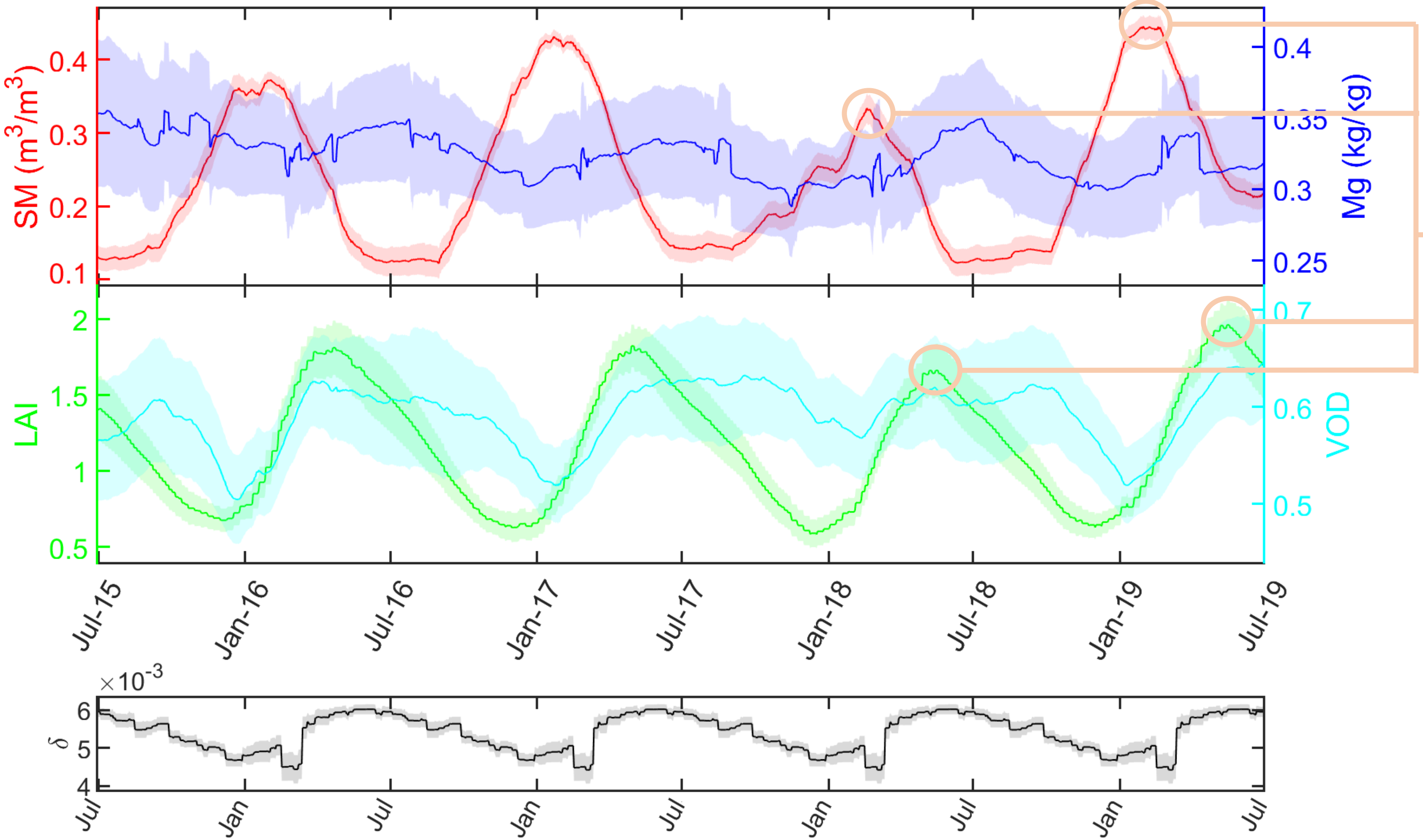


Dry (wet) years could be linked to low (high) LAI values. Future work: study relationships of SM-LAI-Mg anomalies.

- ❖ Increasing SM precedes leaf growth (LAI) and structure changes (δ).
- ❖ Mg increases after LAI-δ peaks, suggesting water uptake after leaves growth.
- ❖ VOD high plateau during LAI & Mg maxima affirming double sensitivity of VOD (biomass & plant water)

# 5. Conclusions and future work

### Developed datasets

- A new VH dataset from ICESat-2 has been presented.
- Dynamic vegetation volume fraction ($\delta$) to capture changes in the vegetation structure.

### California study case: first comparisons of Mg with complementary datasets

- Greater Mg dynamics in semi-arid regions (e.g., Sahel).
- Comparison of Mg with soil and plant time-series are consistent with water fluxes in the SPC.

### Future work

- Including the atmosphere layer (vapor pressure deficit; VPD) for a complete SPAC analysis.
- Studying lag-correlations among SM, Mg, VPD and LAI-VOD to study SPAC water fluxes and plant responses.

# References


- Beck, H. E., Zimmermann, N. E., McVicar, T. R., Vergopolan, N., Berg, A., & Wood, E. F. (2018). Present and future Köppen-Geiger climate classification maps at 1-km resolution. Scientific data, 5, 180214.
- Fink, A., Jagdhuber, T., Piles, M., Grant, J., Baur, M., Link, M., & Entekhabi, D. (2018, July). Estimating gravimetric moisture of vegetation using an attenuation-based multi-sensor approach. In IGARSS 2018-2018 IEEE International Geoscience and Remote Sensing Symposium (pp. 353-356). IEEE.
- Konings, A. G., Piles, M., Rötzer, K., McColl, K. A., Chan, S. K., & Entekhabi, D. (2016). Vegetation optical depth and scattering albedo retrieval using time series of dual-polarized L-band radiometer observations. Remote sensing of environment, 172, 178-189.
- Meyer, T., Jagdhuber, T., Piles, M., Fink, A., Grant, J., Vereecken, H., & Jonard, F. (2019). Estimating gravimetric water content of a winter wheat field from L-band vegetation optical depth. Remote Sensing, 11(20), 2353.
- Simard, M., Pinto, N., Fisher, J. B., & Baccini, A. (2011). Mapping forest canopy height globally with spaceborne lidar. Journal of Geophysical Research: Biogeosciences, 116(G4).
- Ulaby, F. T., & El-Rayes, M. A. (1987). Microwave dielectric spectrum of vegetation-Part II: Dual-dispersion model. IEEE Transactions on Geoscience and Remote Sensing, (5), 550-557.

# Thank you!

#shareEGU20

@DChaparro_EO

EGU General Assembly 2020